MATHEMATICAL ENGINEERING
TECHNICAL REPORTS

Self-Organizing Hexagons for Core–Periphery Models: Central Place Theory and Group Theory

Kiyohiro IKEDA, Kazuo MUROTA,
Takashi AKAMATSU, Tatsuhito KONO,
Yuki TAKAYAMA

METR 2011–24 July 2011

DEPARTMENT OF MATHEMATICAL INFORMATICS
GRADUATE SCHOOL OF INFORMATION SCIENCE AND TECHNOLOGY
THE UNIVERSITY OF TOKYO
BUNKYO-KU, TOKYO 113-8656, JAPAN

WWW page: http://www.keisu.t.u-tokyo.ac.jp/research/techrep/index.html

Self-Organizing Hexagons for Core–Periphery Models: Central Place Theory and Group Theory

Kiyohiro Ikeda[*] [†], Kazuo Murota[‡]
Takashi Akamatsu[§], Tatsuhito Kono[¶], Yuki Takayama[‖]

July 19, 2011

Abstract

Self-organization of agglomeration patterns for core–periphery models in new economic geography is investigated through dual viewpoints of central place theory and group-theoretic bifurcation theory. A system of uniformly-distributed places is modeled by a finite hexagonal lattice with periodic boundaries. Possible agglomeration patterns on this lattice predicted by group-theoretic bifurcation theory are hexagonal distributions of various sizes. The existence of the hexagonal distributions for the hexagonal lattice is ensured and their stability is investigated by the comparative static bifurcation analysis with respect to transport costs. These distributions are the ones which were envisaged by central place theory in economic geography based on a normative and geometrical approach, and were also inferred to emerge by Krugman (1996) in new economic geography for a core–periphery model in two dimensions.

Keywords: bifurcation, central place theory, core–periphery models, group-theoretic bifurcation theory, hexagons, new economic geography, self-organization

[*]Correspondence author: Fax:+81-22-795-7418, ikeda@civil.tohoku.ac.jp
[†]Department of Civil and Environmental Engineering, Tohoku University, Aoba 6-6-06, Sendai 980-8579, Japan
[‡]Department of Mathematical Informatics, University of Tokyo, Tokyo 113-8656, Japan
[§]School of Information Sciences, Tohoku University, Aoba 6-6-06, Sendai 980-8579, Japan
[¶]School of Information Sciences, Tohoku University, Aoba 6-3-09, Sendai 980-8579, Japan
[‖]Graduate School of Science and Engineering, Ehime University, Bunkyo-cho 3, Matsuyama 790-8577, Japan

1 Introduction

Self-organization of hexagonal population distributions[1] from a uniformly inhabited state was envisioned by central place theory in economic geography based on a normative and geometrical approach. In new economic geography, it was inferred to emerge by Krugman (1996) [29] for core–periphery models in two dimensions. In this paper, we show the existence of such distributions for these models theoretically and demonstrate their existence computationally based on an interdisciplinary study synthesizing three independent mainstreams: central place theory, new economic geography, and group-theoretic bifurcation theory.

In central place theory of economic geography,[2] self-organization of hexagonal market areas of three kinds shown in Fig. 1 was proposed by Christaller (1966) [9] based on market, traffic, and administrative principles. The ten smallest hexagons were presented as fundamental sizes of market areas by Lösch (1954) [30]. The assemblage of hexagonal market area with different sizes is expected to produce hierarchical hexagonal distributions of the population of places (cities, towns, villages, etc.). This theory is accepted by geographers to present a deductive base for the study of patterns of location. Yet it is based on a normative and geometrical approach, and is not derived from market equilibrium conditions.[3]

In new economic geography, based on a full-fledged general equilibrium approach, Krugman (1991) [27] developed a core–periphery model, and demonstrated that bifurcation serves as a catalyst to engender agglomeration of population out of uniformly distributed state. This model expressed the microeconomic underpinning of the spatial economic agglomeration, introduced the Dixit–Stiglitz (1977) [14] model of monopolistic competition into spatial economics, and provided a new framework to explain interactions occurring among increasing returns, transportation costs, and factor mobility. Thereafter, new economic geography models sprung up worldwide, as reviewed in several books, such as Fujita et al. (1999) [18], Brakman et al. (2001) [7], Baldwin et al. (2003) [3], and Combes et al. (2008) [11].

Agglomeration patterns vary with models and with spatial configurations:

- The two-city model is studied extensively by virtue of its analytical tractability. Two identical symmetric cities are in a stable state with high transport costs, and when the costs are reduced to a certain level, a bifurcation triggers a concentration to a single city by breaking the symmetry. The tomahawk bifurcation that triggers a spontaneous concentration was observed, e.g., in Krugman (1991) [27] and Fujita et al. (1999) [18] for the Krugman model, and in Forslid and Ottaviano (2003) [16] for an analytically solvable model. A stable non-trivial equilibrium branching from a supercritical pitchfork was observed by Pflüger (2004) [35] for a simple, analytically-solvable model.

[1]See, e.g., Clarke and Wilson (1985) [10] and Munz and Weidlich (1990) [33] for early studies of self-organizing patterns in geography and regional science.

[2]For books and reviews on central place theory, see, for example, Lösch (1954) [30], Isard (1975) [26], Beavon (1977) [4], and Dicken and Lloyd (1990) [12].

[3]Fujita et al. (1999, p.27) [18] stated "Unfortunately, as soon as one begins to think hard about central place theory one realizes that it does not quite hang together as an economic model. $\cdots$ Christaller suggested the plausibility of a hierarchical structure; he gave no account of how individual actions would produce such a hierarchy $\cdots$"

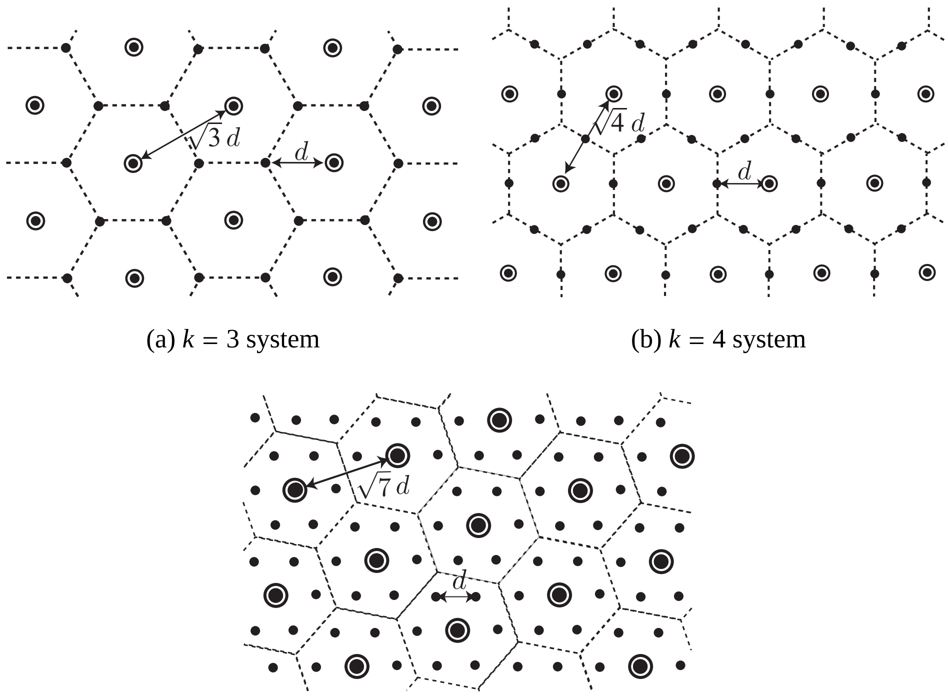

(a) $k = 3$ system

(b) $k = 4$ system

(c) $k = 7$ system

Figure 1: Three systems predicted by Christaller (the area of a circle indicates the size of population)

Yet economic agglomerations, in reality, can take place at more than two locations, as stated by Behrens and Thisse (2007) [5],[4] and as corroborated by empirical evidence (Bosker et al., 2010 [6]).

- Racetrack economy, which represents a system of initially identical places that spread uniformly around the circumference of a circle, has come to be utilized as a spatial platform. A numerical simulation including 12 symmetric cities of equal size revealed that the symmetric equilibrium often becomes unstable (Krugman, 1993 [28]). Fujita et al. (1999) [18] identified the emergence of several spatial frequencies by a local analysis (linearized eigenproblem) of the racetrack economy. Picard and Tabuchi (2010) [36] studied agglomeration to a finite number of places or atomic cities. A characteristic process of spatial agglomeration, called *spatial period-doubling bifurcation cascade*, was observed for 2^k places (k is a positive integer) in Tabuchi and Thisse (2011) [41], Akamatsu et al. (2009) [1], and Ikeda et al. (2010) [23]. In this cascade, 2^k identical places undergo a sequence of concentrations into 2^{k-1} identical places, 2^{k-2} identical places, . . ., en route to the emergence of complete agglomeration into a single place, megalopolis.

[4] Behrens and Thisse (2007; pp.461–462) [5] stated: "in multi-regional systems the so-called 'three-ness effect' enters the picture and introduces complex feedbacks into the models, which significantly complicates the analysis. Dealing with these spatial interdependencies constitutes one of the main theoretical and empirical challenges NEG and regional economics will surely have to face in the future."

However, the hexagonal patterns in central place theory have yet to be found for core–periphery models as stated by Krugman (1996; p.91) [29], based on the study of a racetrack economy, as:

> I have demonstrated the emergence of a regular lattice only for a one-dimensional economy, but I have no doubt that a better mathematician could show that a system of hexagonal market areas will emerge in two dimensions.

A clue for a mathematical procedure for this purpose can be found in nonlinear mathematics and physics, in which the emergence of patterns out of uniformity has been treated as an important subject, called pattern formation. Sattinger (1978) [38] elucidated the mechanism of the self-organization of hexagonal patterns by group-theoretic bifurcation analysis under a simplifying assumption that solutions are doubly periodic with respect to a hexagonal lattice. Hexagonal bifurcating patterns were found by the analysis on the hexagonal lattice (Buzano and Golubitsky, 1983 [8]).

An attempt to explain the mechanism of the self-organization of Lösch's ten smallest hexagons in light of group-theoretic bifurcation theory was conducted by Ikeda et al. (2011) [25]. As a spatial platform, a rhombic domain with periodic boundaries comprising uniformly distributed $n \times n$ places that are connected by roads of the same length forming a finite hexagonal lattice was employed. This is based on the so called *infinite-periodic-domain approximation* which assumes that the finite lattice is periodically repeated spatially to cover an infinite two-dimensional domain (Ikeda and Murota, 2010, Chapter 14 [24]). Lösch's ten hexagonal distributions are guaranteed to be existent by equivariant bifurcation analysis, and some of them are obtained by computational analysis for the FO model (Forslid and Ottaviano, 2003 [16]) that replaces the production function of Krugman with that of Flam and Helpman (1987) [15]. Thus the mathematical mechanism for the self-organization of hexagonal patterns has been untangled.

The objective of this paper is to demonstrate the emergence of hexagonal population distributions of Christaller's $k = 3, 4, 7$ systems for core–periphery models on the hexagonal lattice. The mathematical results in Ikeda et al. (2011) [25] are, in principle, applicable to core–periphery models of various kinds. Yet the occurrence and non-occurrence of bifurcations that engender hexagonal patterns of interest are dependent on individual cases for individual models and must be investigated for each case. To show the model independence of the existence of hexagonal distributions, we employ core–periphery models of two kinds that are readily formulated for a system of cities (Section 2): (a) the aforementioned FO model and (b) the Pf model by Pflüger, 2004 [35] that replaces, in addition to the production function, the utility function of Krugman with that of the international trade model of Martin and Rogers (1995) [31]. In the computational analysis conducted in this paper (Section 4), the two models turn out to display quantitatively different but qualitatively identical behaviors. Hexagonal distributions of population that give Christaller's three systems in Fig. 1 are found to emerge by computational bifurcation analysis for a system of 42×42 places, and the stability of these distributions is investigated. It is a topic for future to deal with other important core–periphery models to further investigate the model independence.

The economic and geographical implications of the resulting hexagonal distributions are investigated for Christaller's $k = 3, 4, 7$ systems. The ratio of the number of first-level centers with the largest population to that of the second-level centers with the second largest population is studied on the basis of central place theory. The dependence of stability of solutions on the transport cost is highlighted as the economic implication drawn through the present study. Consequently, this paper presents a step toward uniting central place theory and core–periphery models in light of group-theoretic bifurcation theory.

This paper is organized as follows: The two core–periphery models are presented in Section 2. A system of places that is uniformly spread on an infinite hexagonal lattice in two dimensions is modeled, and its bifurcation mechanism producing hexagonal distributions is predicted by group-theoretic bifurcation theory in Section 3. Computational bifurcation analysis of the hexagonal lattice is conducted in Section 4 to find bifurcated patterns that represent Christaller's hexagonal market areas. Details of the equivariant bifurcation analysis are presented in the Appendix.

2 Core–periphery models

In the present study, we use two analytically-solvable core–periphery models that are readily formulated for a system of places:

i) FO model (Forslid and Ottaviano, 2003 [16]) that replaces the production function of Krugman with that of Flam and Helpman (1987) [15].

ii) Pf model (Pflüger, 2004 [35]) that replaces, in addition to the production function, the utility function of Krugman with that of the international trade model of Martin and Rogers (1995) [31].

After presenting basic assumptions in §2.1, we describe the short-run equilibrium in §2.2, and define the long-run equilibrium in §2.3.

2.1 Basic assumptions

The economy is composed of K regions (labeled $i = 1, \ldots, K$), two factors of production (skilled and unskilled labor), and two sectors (agriculture A and manufacturing M). There are H skilled and $L = K$ unskilled workers, who consume two final goods, namely, horizontally differentiated M-sector goods and homogeneous A-sector goods, and supply one unit of his type of labor inelastically. Skilled workers are mobile across regions. The number of skilled workers in region i is denoted by h_i, and the equality

$$H = \sum_{i=1}^{K} h_i \tag{1}$$

is satisfied. Unskilled workers are immobile and equally distributed across all places with the unit density (i.e., $L = 1 \times K$). Hence the population in place i is equal to $h_i + 1$.

Preferences U over the M- and A-sector goods are identical across individuals. The utility of an individual in place i is

$$\text{[FO model}^5\text{]} \quad U(C_i^{\mathrm{M}}, C_i^{\mathrm{A}}) = \mu \ln C_i^{\mathrm{M}} + (1-\mu) \ln C_i^{\mathrm{A}} \qquad (0 < \mu < 1), \tag{2a}$$

$$\text{[Pf model]} \quad U(C_i^{\mathrm{M}}, C_i^{\mathrm{A}}) = \mu \ln C_i^{\mathrm{M}} + C_i^{\mathrm{A}} \qquad (\mu > 0), \tag{2b}$$

where μ is a constant parameter, C_i^{A} is the consumption of the A-sector product in place i, and C_i^{M} is the manufacturing aggregate in place i and is defined as

$$C_i^{\mathrm{M}} \equiv \left(\sum_j \int_0^{n_j} q_{ji}(\ell)^{(\sigma-1)/\sigma} d\ell \right)^{\sigma/(\sigma-1)},$$

where $q_{ji}(\ell)$ is the consumption in place i of a variety $\ell \in [0, n_j]$ produced in place j, n_j is the continuum range of varieties produced in place j, often called the

[5] We take logarithms of the Forslid and Ottaviano (2003) [16] type (i.e., Cobb–Douglas-type) utility function to facilitate the analysis. This transformation has no influence on the properties of the model.

number of available varieties, and $\sigma > 1$ is the constant elasticity of substitution between any two varieties. The budget constraint is given as

$$p_i^{\mathrm{A}} C_i^{\mathrm{A}} + \sum_j \int_0^{n_j} p_{ji}(\ell) q_{ji}(\ell) d\ell = Y_i, \tag{3}$$

where p_i^{A} is the price of A-sector goods in place i, $p_{ji}(\ell)$ is the price of a variety ℓ in place i produced in place j and Y_i is the income of an individual in place i. The incomes (wages) of the skilled worker and the unskilled worker are represented, respectively, by w_i and w_i^{L}.

An individual in place i maximizes (2) subject to (3). This yields the following demand functions:

$$\text{[FO model]} \quad C_i^{\mathrm{A}} = (1-\mu)\frac{Y_i}{p_i^{\mathrm{A}}}, \quad C_i^{\mathrm{M}} = \mu \frac{Y_i}{\rho_i}, \quad q_{ji}(\ell) = \mu \frac{p_i^{\mathrm{A}} \rho_i^{\sigma-1} Y_i}{p_{ji}(\ell)^{\sigma}}, \tag{4a}$$

$$\text{[Pf model]} \quad C_i^{\mathrm{A}} = \frac{Y_i}{p_i^{\mathrm{A}}} - \mu, \quad C_i^{\mathrm{M}} = \mu \frac{p_i^{\mathrm{A}}}{\rho_i}, \quad q_{ji}(\ell) = \mu \frac{p_i^{\mathrm{A}} \rho_i^{\sigma-1}}{p_{ji}(\ell)^{\sigma}}, \tag{4b}$$

where ρ_i denotes the price index of the differentiated product in place i, which is

$$\rho_i = \left(\sum_j \int_0^{n_j} p_{ji}(\ell)^{1-\sigma} d\ell \right)^{1/(1-\sigma)}. \tag{5}$$

Since the total income and population in place i are $w_i h_i + w_i^{\mathrm{L}}$ and $h_i + 1$, respectively, we have the total demand $Q_{ji}(\ell)$ in place i for a variety ℓ produced in place j:

$$\text{[FO model]} \quad Q_{ji}(\ell) = \mu \frac{p_i^{\mathrm{A}} \rho_i^{\sigma-1}}{p_{ji}(\ell)^{\sigma}} (w_i h_i + w_i^{\mathrm{L}}), \tag{6a}$$

$$\text{[Pf model]} \quad Q_{ji}(\ell) = \mu \frac{p_i^{\mathrm{A}} \rho_i^{\sigma-1}}{p_{ji}(\ell)^{\sigma}} (h_i + 1). \tag{6b}$$

The A-sector is perfectly competitive and produces homogeneous goods under constant returns to scale technology, which requires one unit of unskilled labor in order to produce one unit of output. For simplicity, we assume that the A-sector goods are transported freely between places and that they are chosen as the numéraire. These assumptions mean that, in equilibrium, the wage of an unskilled worker w_i^{L} is equal to the price of A-sector goods in all places (i.e., $p_i^{\mathrm{A}} = w_i^{\mathrm{L}} = 1$ for each $i = 1, \ldots, K$).

The M-sector output is produced under increasing returns to scale technology and Dixit-Stiglitz monopolistic competition. A firm incurs a fixed input requirement of α units of skilled labor and a marginal input requirement of β units of unskilled labor. Given the fixed input requirement α, the skilled labor market clearing implies that, in equilibrium, the number of firms in place i is determined by $n_i = h_i/\alpha$. An M-sector firm located in place i chooses $(p_{ij}(\ell) \mid j = 1, \ldots, K)$ that maximizes its profit

$$\Pi_i(\ell) = \sum_j p_{ij}(\ell) Q_{ij}(\ell) - (\alpha w_i + \beta x_i(\ell)),$$

where $x_i(\ell)$ is the total supply. The transportation costs for M-sector goods are assumed to take the iceberg form. That is, for each unit of M-sector goods transported from place i to place $j \neq i$, only a fraction $1/\phi_{ij} < 1$ arrives. Consequently, the total supply $x_i(\ell)$ is given as

$$x_i(\ell) = \sum_j \phi_{ij} Q_{ij}(\ell). \tag{7}$$

To put it concretely, we define the transport cost ϕ_{ij} between the two places i and j as

$$\phi_{ij} = \exp(\tau D_{ij}), \tag{8}$$

where τ is the transport parameter and D_{ij} represents the shortest distance between places i and j.

Since we have a continuum of firms, each firm is negligible in the sense that its action has no impact on the market (i.e., the price indices). Therefore, the first-order condition for profit maximization gives

$$p_{ij}(\ell) = \frac{\sigma\beta}{\sigma - 1}\phi_{ij}. \tag{9}$$

This expression implies that the price of the M-sector product does not depend on variety ℓ, so that $Q_{ij}(\ell)$ and $x_i(\ell)$ do not depend on ℓ. Therefore, we describe these variables without the argument ℓ. Substituting (9) into (5), we have the price index

$$\rho_i = \frac{\sigma\beta}{\sigma - 1}\left(\frac{1}{\alpha}\sum_j h_j d_{ji}\right)^{1/(1-\sigma)}, \tag{10}$$

where $d_{ji} = \phi_{ji}^{1-\sigma}$ is a spatial discounting factor between places j and i; from (6) and (10), d_{ji} is obtained as $(p_{ji}Q_{ji})/(p_{ii}Q_{ii})$, which means that d_{ji} is the ratio of total expenditure in place i for each M-sector product produced in place j to the expenditure for a domestic product.

2.2 Short-run equilibrium

In the short run, skilled workers are immobile between places, i.e., their spatial distribution ($\boldsymbol{h} = (h_i) \in \mathbb{R}^K$) is assumed to be given. The short-run equilibrium conditions consist of the M-sector goods market clearing condition and the zero-profit condition because of the free entry and exit of firms. The former condition can be written as (7). The latter condition requires that the operating profit of a firm is absorbed entirely by the wage bill of its skilled workers:

$$w_i(\boldsymbol{h}, \tau) = \frac{1}{\alpha}\left\{\sum_j p_{ij} Q_{ij}(\boldsymbol{h}, \tau) - \beta x_i(\boldsymbol{h}, \tau)\right\}. \tag{11}$$

Substituting (6), (7), (9), and (10) into (11), we have the short-run equilibrium wage:

$$\text{[FO model]} \quad w_i(\boldsymbol{h}, \tau) = \frac{\mu}{\sigma}\sum_j \frac{d_{ij}}{\Delta_j(\boldsymbol{h}, \tau)}(w_j(\boldsymbol{h}, \tau)h_j + 1), \tag{12a}$$

$$\text{[Pf model]} \quad w_i(\boldsymbol{h}, \tau) = \frac{\mu}{\sigma}\sum_j \frac{d_{ij}}{\Delta_j(\boldsymbol{h}, \tau)}(h_j + 1), \tag{12b}$$

where $\Delta_j(\boldsymbol{h}, \tau) \equiv \sum_k d_{kj} h_k$ denotes the market size of the M-sector in place j. Consequently, $d_{ij}/\Delta_j(\boldsymbol{h}, \tau)$ defines the market share in place j of each M-sector product produced in place i.

The indirect utility $v_i(\boldsymbol{h}, \tau)$ is obtained by substituting (4), (10), and (12) into (2):[6]

$$\text{[FO model]} \quad v_i(\boldsymbol{h}, \tau) = S_i(\boldsymbol{h}, \tau) + \ln[w_i(\boldsymbol{h}, \tau)], \tag{13a}$$

$$\text{[Pf model]} \quad v_i(\boldsymbol{h}, \tau) = S_i(\boldsymbol{h}, \tau) + w_i(\boldsymbol{h}, \tau), \tag{13b}$$

where

$$S_i(\boldsymbol{h}, \tau) \equiv \mu(\sigma - 1)^{-1} \ln \Delta_i(\boldsymbol{h}, \tau).$$

2.3 Adjustment process and long-run equilibrium

In the long run, the skilled workers are inter-regionally mobile. They are assumed to be heterogeneous in their preferences for location choice. That is, the indirect utility for an individual s in place i is expressed as

$$v_i^{(s)}(\boldsymbol{h}, \tau) = v_i(\boldsymbol{h}, \tau) + \epsilon_i^{(s)}.$$

In this equation, $\epsilon_i^{(s)}$, which is distributed continuously across individuals, denotes the utility representing the idiosyncratic taste for residential location.

We present the dynamics of the migration of the skilled workers to define the long-run equilibrium. We assume that at each time period t, the opportunity for skilled workers to migrate emerges according to an independent Poisson process with arrival rate λ. That is, for each time interval $[t, t + dt)$, a fraction λdt of skilled workers have the opportunity to migrate. Given an opportunity at time t, each worker chooses the place that provides the highest indirect utility $v_i^{(s)}(\boldsymbol{h}, \tau)$, which depends on the current distribution $\boldsymbol{h} = \boldsymbol{h}(t)$. The fraction of skilled workers who choose place i under distribution $\boldsymbol{h}$ is $P_i(\boldsymbol{v}(\boldsymbol{h}), \tau)$, where

$$P_i(\boldsymbol{v}, \tau) = \Pr[v_i^{(s)} > v_j^{(s)}, \ \forall j \neq i].$$

Therefore, we have

$$h_i(t + dt) = (1 - \lambda dt) h_i(t) + \lambda dt H P_i(\boldsymbol{v}(\boldsymbol{h}(t)), \tau).$$

By normalizing the unit of time so that $\lambda = 1$, we obtain the following adjustment process:

$$\dot{\boldsymbol{h}}(t) = \boldsymbol{F}(\boldsymbol{h}(t), \tau) \equiv H\boldsymbol{P}(\boldsymbol{v}(\boldsymbol{h}(t)), \tau) - \boldsymbol{h}(t), \tag{14}$$

where $\dot{\boldsymbol{h}}(t)$ denotes the time derivative of $\boldsymbol{h}(t)$, and $\boldsymbol{P}(\boldsymbol{v}(\boldsymbol{h}), \tau) = (P_i(\boldsymbol{v}(\boldsymbol{h}), \tau))$. For the specific functional form of $P_i(\boldsymbol{v}, \tau)$, we use the logit choice function:

$$P_i(\boldsymbol{v}, \tau) \equiv \frac{\exp[\theta v_i]}{\sum_j \exp[\theta v_j]}, \tag{15}$$

[6]We ignore the constant terms, which have no influence on the results below.

where $\theta \in (0, \infty)$ is the parameter denoting the inverse of variance of the idiosyncratic tastes. This implies the assumption that the distributions of $(\epsilon_i^{(s)})$'s are Gumbel distributions, which are identical and independent across places (e.g., McFadden, 1974 [32]; Anderson et al., 1992 [2]). The adjustment process described by (14) and (15) is the logit dynamics, which has been studied in evolutionary game theory (e.g., Fudenberg and Levine, 1998 [17]; Hofbauer and Sandholm, 2007 [22]; Sandholm, 2010 [37]).

Next, we define the long-run equilibrium, which is a stationary point of the adjustment process of (14).

Definition 2.1. The long-run equilibrium is defined as the distribution $\boldsymbol{h}^*$ that satisfies

$$\boldsymbol{F}(\boldsymbol{h}^*, \tau) \equiv H\boldsymbol{P}(\boldsymbol{v}(\boldsymbol{h}^*), \tau) - \boldsymbol{h}^* = \boldsymbol{0}. \tag{16}$$

The heterogeneous worker case includes the conventional homogeneous worker case. Indeed, when $\theta \to \infty$, the condition given in (16) reduces to that for the homogeneous worker case:

$$\begin{cases} V^* - v_i(\boldsymbol{h}^*, \tau) = 0 & \text{if} \quad h_i^* > 0, \\ V^* - v_i(\boldsymbol{h}^*, \tau) \geq 0 & \text{if} \quad h_i^* = 0, \end{cases}$$

where V^* denotes the equilibrium utility.

3 System of places on a finite hexagonal lattice and their bifurcation

A finite hexagonal lattice is introduced as the spatial platform of the core–periphery models presented in Section 2. Christaller's hexagonal distributions are reviewed in §3.1 based on Christaller (1966) [9] and Dicken and Lloyd (1990) [12]. After introducing the hexagonal lattice in §3.2, we prescribe two-dimensional periodicity and hexagonal distributions in §3.3, and study possible bifurcations of the hexagonal lattice in §3.4.

3.1 Christaller's hexagonal distributions: review

In central place theory, a completely homogeneous infinite two-dimensional land surface is introduced based on the several simplifying assumptions. The assumptions are summarized as:

(i) The land surface is completely flat and homogeneous in every aspect. It is, in technical terms, an *isotropic* plain.

(ii) Movement can occur in all directions with equal ease and that there is only one type of transportation.

(iii) The plain is limitless or unbounded, so that we do not have to deal with the many complexities that tend to occur at boundaries.

(iv) The population is spread evenly over the plain.

When there are a number of productions of the same good on that homogeneous plain, the best solution that provides maximum coverage from a minimum number of supply points is a uniform hexagonal lattice of production centers. For production of bundles of goods, there appear many levels in the hierarchy of central places. Dicken and Lloyd (1990, pp.28) [12]) stated:

> Christaller's model, then, implies a fixed relationship between each level in the hierarchy. This relationship is known as a k value (k meaning a constant) and indicates that each center dominates a discrete number of lower-order centers and market areas in addition to its own.

The hexagonal market areas of three kinds shown in Fig. 1 are called $k = 3$ system, $k = 4$ system, and $k = 7$ system, which are respectively based on market, traffic, and administrative principles (Christaller, 1966, pp.74–77 [9]; Dicken and Lloyd, 1990, Chapter 1 [12]). The k value has a geometrical implication in that $\sqrt{k}$ is proportional to the distance T between the first-level centers with the largest population. We, accordingly, has a key formula

$$T/d = \sqrt{k}, \quad (k = 3, 4, 7), \tag{17}$$

where d is the distance between two neighboring places. The spatial period T represents the radius of hexagons.

A hierarchy of places with different levels exists in the market area governed by the highest-level (first-level) center with the largest population. Such a hierarchy is often called, the first-level center, the second-level center, and so on.[7] When only the first-level and the second-level centers are existent, it is called two-level hierarchy. It is called $N_{\max}$-level hierarchy when up to the $N_{\max}$-th hierarchy is existent.

The number N_j of the j-th level centers dominated by the first level center is given as (Christaller, 1966, p.67 [9]):

$$N_1 : N_2 : N_3 : \cdots = 1 : 2 : 6 : 18 : 54 : 162 \cdots \quad \text{for } k = 3 \text{ system,}$$

and as (Dicken and Lloyd, 1990, Chapter 1 [12]):

$$N_1 : N_2 : N_3 : \cdots = 1 : 3 : 12 : 48 : 192 \cdots \quad \text{for } k = 4 \text{ system.}$$

It is possible to arrive at a pertinent recurrence formula

$$N_1 = 1, \quad N_j = k^{j-1} - k^{j-2}, \quad (j = 2, 3, \ldots, N_{\max};\ k = 3, 4, 7). \tag{18}$$

In this paper, we deal only with two-level hierarchy with $N_{\max} = 2$.

3.2 Hexagonal lattice

The infinite two-dimensional domain that is used in central place theory is incompatible with a naive analysis for the core–periphery models, which are formulated for a finite number of places in a finite domain. As a remedy, we introduce a finite hexagonal lattice[8] with periodic boundaries comprising a system of uniformly distributed $n \times n$ places. A place is allocated at each node of the $n \times n$ hexagonal lattice, expressed by

$$\boldsymbol{p} = n_1 \boldsymbol{\ell}_1 + n_2 \boldsymbol{\ell}_2, \quad (n_1, n_2 = 1, \ldots, n),$$

where $\boldsymbol{\ell}_1 = (d, 0)^\top$ and $\boldsymbol{\ell}_2 = (-d/2, d\sqrt{3}/2)^\top$ are oblique basis vectors. Two neighboring places are connected by a straight road with the nominal length d. See Fig. 2(a) for an example of 4×4 hexagonal lattice.

To express the infiniteness, we impose periodic boundary conditions[9] for the hexagonal lattice, and then this lattice can be repeated spatially to cover an infinite two-dimensional domain. See Fig. 2(b) for an example of $n = 4$ to illustrate how the places at the boundaries are connected by roads. By virtue of these boundaries, every place in the hexagonal lattice is surrounded by the same hexagonal transportation network. The lattice can satisfy Assumptions (i), (ii), and (iii) in

[7] Such a hierarchy is also called metropolis, city, town, village, hamlet; or A-level center, B-level center, C-level center, and so on.

[8] There exist planar lattices of five kinds, rhombic, square, hexagonal, rectangular, and oblique (Golubitsky and Stewart, 2002 [20]). The hexagonal lattice (net of hexagons) is said to be superior to the square lattice (Lösch, 1954, pp.133–134 [30]), and is often called *basic lattice* (Beavon 1977, p.83, [4]).

[9] By the assumption of periodic boundaries, the finite lattice is periodically repeated spatially to cover an infinite two-dimensional domain.

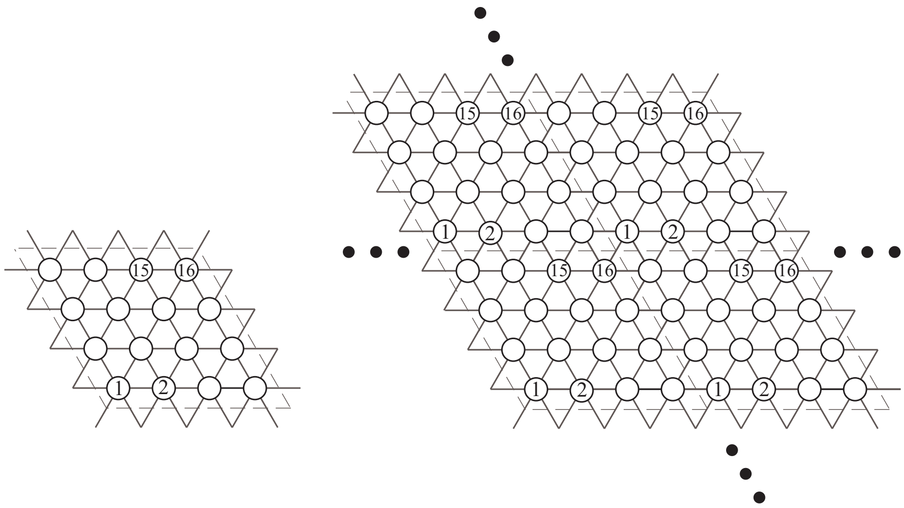

(a) 4×4 hexagonal lattice (b) Spatially repeated 4×4 hexagonal lattices

Figure 2: A system of places in a 4×4 hexagonal lattice with periodic boundaries

§3.1 in a discretized sense. Assumption (iv) can be satisfied since the uniformly distributed population

$$h_1 = \cdots = h_{n^2} = 1/n^2 \tag{19}$$

of the skilled workers is the pre-bifurcation solution to the governing equation (16) for any value of the transport parameter τ, and this solution is shown to be stable for very large values of τ associated with primitive state of urbanization in Section 4. The hexagonal lattice, accordingly, might be touted as a discretized counterpart of the isotropic plain in central place theory.

3.3 Two-dimensional periodicity and hexagonal distributions

If the population distribution of a system of places (i.e., a subset of nodes) has two-dimensional periodicity, then we can set a pair of independent vectors

$$(\boldsymbol{t}_1, \boldsymbol{t}_2), \tag{20}$$

called the spatial period vectors, such that the system remains invariant under the translations associated with these vectors. The spatial periods (T_1, T_2) are defined as $T_i = \|\boldsymbol{t}_i\|$ $(i = 1, 2)$.

Among possible doubly-periodic distributions, we specifically examine a hexagonal distribution that is described by

$$\boldsymbol{t}_1 = \alpha \boldsymbol{\ell}_1 + \beta \boldsymbol{\ell}_2, \quad \boldsymbol{t}_2 = -\beta \boldsymbol{\ell}_1 + (\alpha - \beta)\boldsymbol{\ell}_2, \quad (\alpha, \beta \in \mathbb{Z}), \tag{21}$$

for which $T_1 = T_2 (\equiv T)$ is satisfied and the angle between $\boldsymbol{t}_1$ and $\boldsymbol{t}_2$ is $2\pi/3$. The associated normalized spatial period is given by

$$T/d = \sqrt{(\alpha - \beta/2)^2 + (\beta\sqrt{3}/2)^2} = \sqrt{\alpha^2 - \alpha\beta + \beta^2}. \tag{22}$$

We consider a positive integer

$$k = \alpha^2 - \alpha\beta + \beta^2,$$

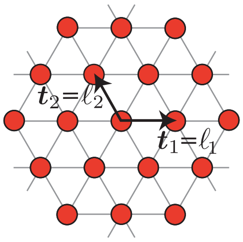

(a) Uniform distribution ($k = 1$)

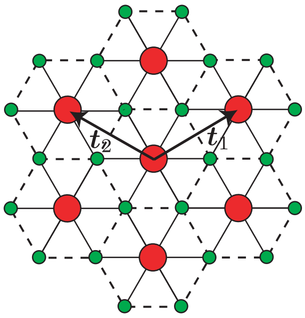

(b) $k = 3$ system

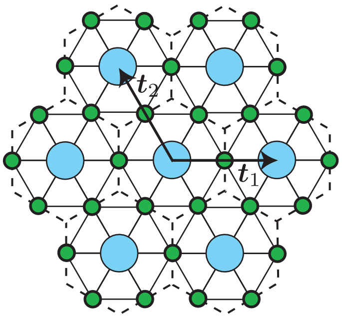

(c) $k = 4$ system

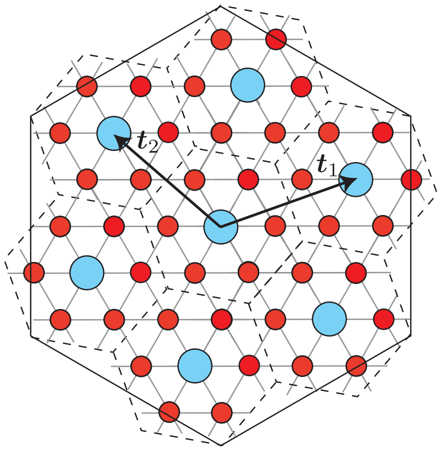

(d) $k = 7$ system

Figure 3: Hexagonal distributions on the hexagonal lattice (Area of the circle represents the size of population)

which can take some specific integer values, such as 1, 3, 4, 7, . . . , and rewrite the normalized spatial period in (22) as

$$T/d = \sqrt{k} \quad (k = 1, 3, 4, 7, \ldots), \tag{23}$$

which lies in the range $1 \leq T/d \leq n$ and take some specific values, such as $\sqrt{1}$, $\sqrt{3}$, $\sqrt{4}$, $\sqrt{7}$, ...

The hexagonal distribution for $k = 1$ corresponds to the uniform distribution in (19) (Fig. 3(a)), and those for other k values as $k = 3$, 4, 7, . . . systems. The values of (α, β) for these systems are not unique in general but are given, for example, as

$$(\alpha, \beta) = \begin{cases} (1, 0): & \text{uniform distribution } (k = 1), \\ (2, 1): & k = 3 \text{ system}, \\ (2, 0): & k = 4 \text{ system}, \\ (3, 1): & k = 7 \text{ system}. \end{cases}$$

We are particularly interested in the three systems associated with $k = 3$, 4, and 7, which correspond to Christaller's $k = 3$, 4, and 7 systems, as depicted in Fig. 3(b)–(d). These three systems are observed in computational bifurcation analysis in Section 4.

3.4 Bifurcating patterns on the hexagonal lattice

Bifurcating patterns on the $n \times n$ hexagonal lattice were studied by equivariant bifurcation theory in Ikeda et al. (2011) [25] to obtain possible hexagonal patterns of agglomeration. The results of this study related to Christaller's $k = 3$, 4, and 7 systems are presented briefly here (see the Appendix for theoretical details).

It is to be noted first that the uniformly distributed population solution $h_1 = \cdots = h_{n^2} = 1/n^2$ of the skilled workers in (19) is the simplest hexagonal distribution. This solution is existent for any value of the transport parameter τ, which is the bifurcation parameter, and serves as the pre-bifurcation solution. There exist bifurcated solutions of various kinds branching from various bifurcation points on the uniformly distributed state. Bifurcations producing Christaller's $k = 3$, 4, and 7 systems are existent for some specific values of the size n of the lattice and the multiplicity M of the bifurcation point.[10] These bifurcations are characterized by the (normalized) spatial period T/d and the spatial period vectors $(\boldsymbol{t}_1, \boldsymbol{t}_2)$ as expounded in Proposition 3.1 below. This proposition turns out to be of great assistance in the computational analysis in Section 4.

Proposition 3.1. (i) *The size n of the lattice and the multiplicity M of the bifurcation point that can potentially engender $k = 3$, 4, and 7 systems from uniformly distributed state are given by*

$$(n, M) = \begin{cases} (3m, 2) & k = 3 \text{ system}, \\ (2m, 3) & k = 4 \text{ system}, \\ (7m, 12) & k = 7 \text{ system}, \end{cases} \tag{24}$$

where $m = 1, 2, \ldots$.

(ii) *The lattice admits all of these three systems as bifurcated solutions only if the lattice size n is a multiple of 42, i.e.,*

$$n = 42m \quad (m = 1, 2, \ldots).$$

(iii) *The bifurcated solutions for $k = 3$, 4, and 7 systems have the spatial period*

$$T/d = \sqrt{k}, \quad (k = 3, 4, 7), \tag{25}$$

in agreement with (17), and have the spatial period vectors

$$(\boldsymbol{t}_1, \boldsymbol{t}_2) = \begin{cases} (2\boldsymbol{\ell}_1 + \boldsymbol{\ell}_2, -\boldsymbol{\ell}_1 + \boldsymbol{\ell}_2), & k = 3 \text{ system}, \\ (2\boldsymbol{\ell}_1, 2\boldsymbol{\ell}_2), & k = 4 \text{ system}, \\ (3\boldsymbol{\ell}_1 + \boldsymbol{\ell}_2, -\boldsymbol{\ell}_1 + 2\boldsymbol{\ell}_2), & k = 7 \text{ system}. \end{cases}$$

□

By Proposition 3.1(iii), we see that the spatial period becomes $\sqrt{k}$-times as large as the unit spatial period for the uniformly populated state.

[10] At a bifurcation point of the governing equation of the lattice, there are M (≥ 1) zero eigenvalues of the Jacobian matrix $\nabla \boldsymbol{F}(\boldsymbol{h}, \tau) \equiv (\partial F_i(\boldsymbol{h}, \tau)/\partial h_j)$ of the governing equation $\boldsymbol{F}(\boldsymbol{h}^*, \tau) \equiv H\boldsymbol{P}(\boldsymbol{v}(\boldsymbol{h}^*), \tau) - \boldsymbol{h}^* = \boldsymbol{0}$ in (16). The number M is called *multiplicity*, and plays a key role in the classification of bifurcation points.

4 Computationally obtained hexagonal distributions

We examine spatial agglomeration patterns of the population of skilled workers among a system of places that spread uniformly on the $n \times n$ hexagonal lattice by the comparative static bifurcation analysis on the governing equation (16) with respect to transport costs. As core–periphery models, the FO model and the Pf model are used (Section 2). Direct bifurcations from uniformly distributed population that produce hexagonal distributions for Christaller's $k = 3$, 4, and 7 systems are respectively investigated in §4.1–§4.3. Dependence of stability of solutions on the transport cost is studied in §4.4.

We use the following parameter values:

- The length d of the road connecting neighboring places is $d = 1/n$ (§3.2).
- The parameter μ of the utility function is $\mu = 0.4$ (§2.1).
- The constant elasticity σ of substitution between any two varieties is $\sigma = 5.0$ (§2.1).
- The total number H of skilled workers is chosen as $H = 42$ (§2.1).
- The inverse θ of variance of the idiosyncratic tastes is $\theta = 1000$ (§2.3).

Recall that the hexagonal distributions for $k = 3$, 4, and 7 systems appear, via direct bifurcations, only for specific values of n (Proposition 3.1(i) in §3.4). We elaborately set $n = 42$, which is the minimum value of n that can engender all of $k = 3$, 4, and 7 systems (Proposition 3.1(ii)).

Recall that the uniformly distributed population $h_1 = \cdots = h_{n^2} = 1/n^2$ in (19) of the skilled workers is the pre-bifurcation solution to the governing equation (16) that exists for any value of the transport parameter τ. The comparative static bifurcation analysis on the governing equation (16) with respect to transport costs is conducted for the system of 42×42 hexagonal lattice as follows:

- Eigenanalysis of the Jacobian matrix $\nabla \boldsymbol{F}(\boldsymbol{h}, \tau) \equiv (\partial F_i(\boldsymbol{h}, \tau)/\partial h_j)$ of the adjustment process of (14) is conducted on the uniform population solution to check the stability of this solution and to find bifurcation points on this solution.
- Bifurcated solutions branching from the uniform population distribution are obtained and their stability is investigated by the eigenanalysis.

Figure 4 depicts solution curves (the maximum population $h_{\max}$ versus the transport parameter τ curves) for the FO and Pf models obtained in this manner, where $h_{\max} = \max(h_1, \ldots, h_K)$ ($K = 42 \times 42$). The uniform population solution corresponds to the horizontal line OO′ at $h_{\max} = H/n^2 = 1/42 \approx 0.024$, which is stable during OA (shown by the solid line). On the line OO′, a number of bifurcation points with the multiplicity $M = 2$, 3, 4, 6, or 12 are existent. Among these bifurcation points, we specifically examine the direct bifurcations from the following three bifurcation points:

- Bifurcation point A with $M = 2$ engendering $k = 3$ system.
- Bifurcation point C with $M = 3$ engendering $k = 4$ system.
- Bifurcation point B with $M = 12$ engendering $k = 7$ system.

4.1 $k = 3$ system

We deal with the FO model first. As can be seen from Fig. 4(a), a bifurcated curve ADE branched at the double bifurcation point A ($M = 2$) on the line OO′ for the uniform population. The curve ADE lost stability at the onset of bifurcation,[11] remained unstable during AD, regained stability at D, and remained stable during DE. Along the curve ADE, $h_{\max}$ increased from 0.024 to 0.071, where $h_{\max} = 0.024$ corresponds to the uniformly distributed state.

The progress of agglomeration observed on the bifurcated curve ADE is shown in Fig. 5(a) for three different stages: bifurcation point A ($h_{\max} = 0.029$), unstable curve AD ($h_{\max} = 0.040$), and stable curve DE ($h_{\max} = 0.071$). The area of a circle indicates the size of the population at the associated place. In view of the sizes of population, these places are classified into:

- The first-level centers (denoted by the large circle).
- The second-level centers (denoted by the small circle).

$h_{\max}$ is equal to the population at a first-level center. We can observe the progress of agglomeration:

- At bifurcation point A ($h_{\max} = 0.029$), the population is uniformly distributed, and there is no distinction between the-first and the second level centers.
- For unstable curve AD ($h_{\max} = 0.040$), the difference of the first-level centers and second-level ones emerges.
- For stable curve DE ($h_{\max} = 0.071$), the population at the second-level centers almost disappears to realize a distinctive domination of the first-level centers over the second-level centers.

Each first-level center is surrounded by six regular-hexagonal second-level centers to display a two-dimensional core–periphery pattern. On each straight line along the hexagonal grid, we can observe repetitions of one first-level center and two second-level centers. This pattern is different from the pre-existing core–periphery patterns:

- For the two-city model, by bifurcation, a place grows to the first-level center and another place shrinks to the second-level center (e.g., Krugman, 1991 [27] and Fujita et al., 1999 [18] for the Krugman model).
- In the racetrack economy, after the spatial period doubling bifurcation, the first-level center and the second-level center appear alternately on the circle, and each first-level center is surrounded by two neighboring second-level centers (Tabuchi and Thisse, 2011 [41], Akamatsu et al., 2009 [1], and Ikeda et al., 2010 [23]).

Such difference indicates the importance of the study of two-dimensional core–periphery patterns.

[11] Such loss of stability at the onset of bifurcation is widely observed for the two-city model of core–periphery models (e.g., Krugman, 1991 [27] and Fujita et al., 1999 [18] for the Krugman model).

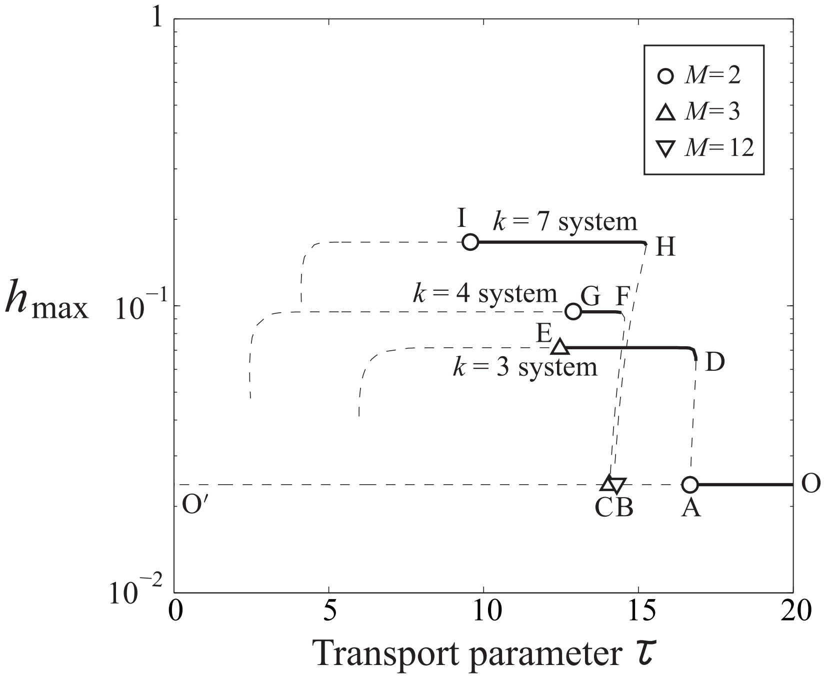

(a) FO model

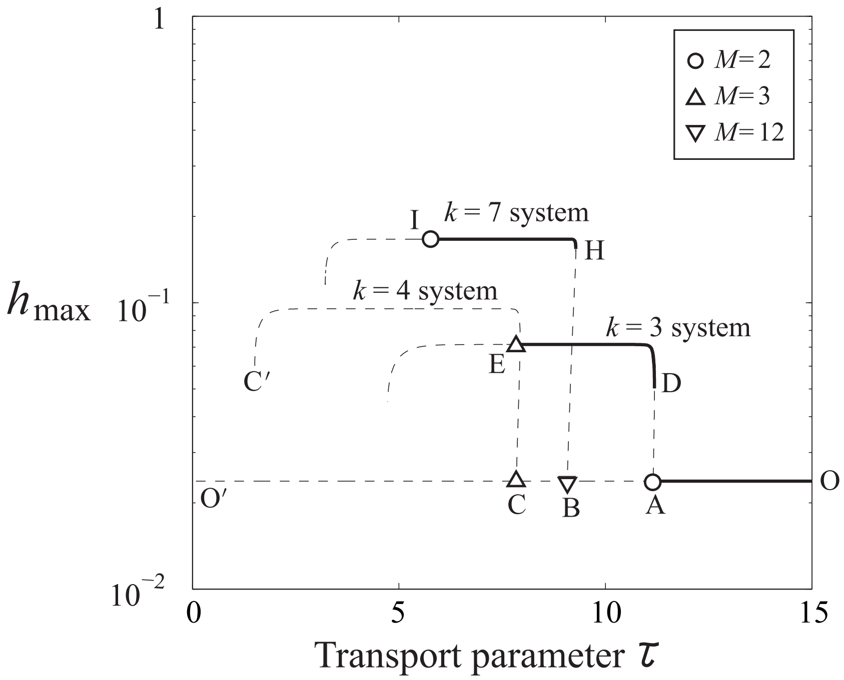

(b) Pf model

Figure 4: Solution curves (the maximum population $h_{\max}$ versus the transport parameter τ curves) for the system of 42×42 places computed for the FO and Pf models (Solid curve: stable, dashed curve: unstable; M is the multiplicity of the bifurcation point)

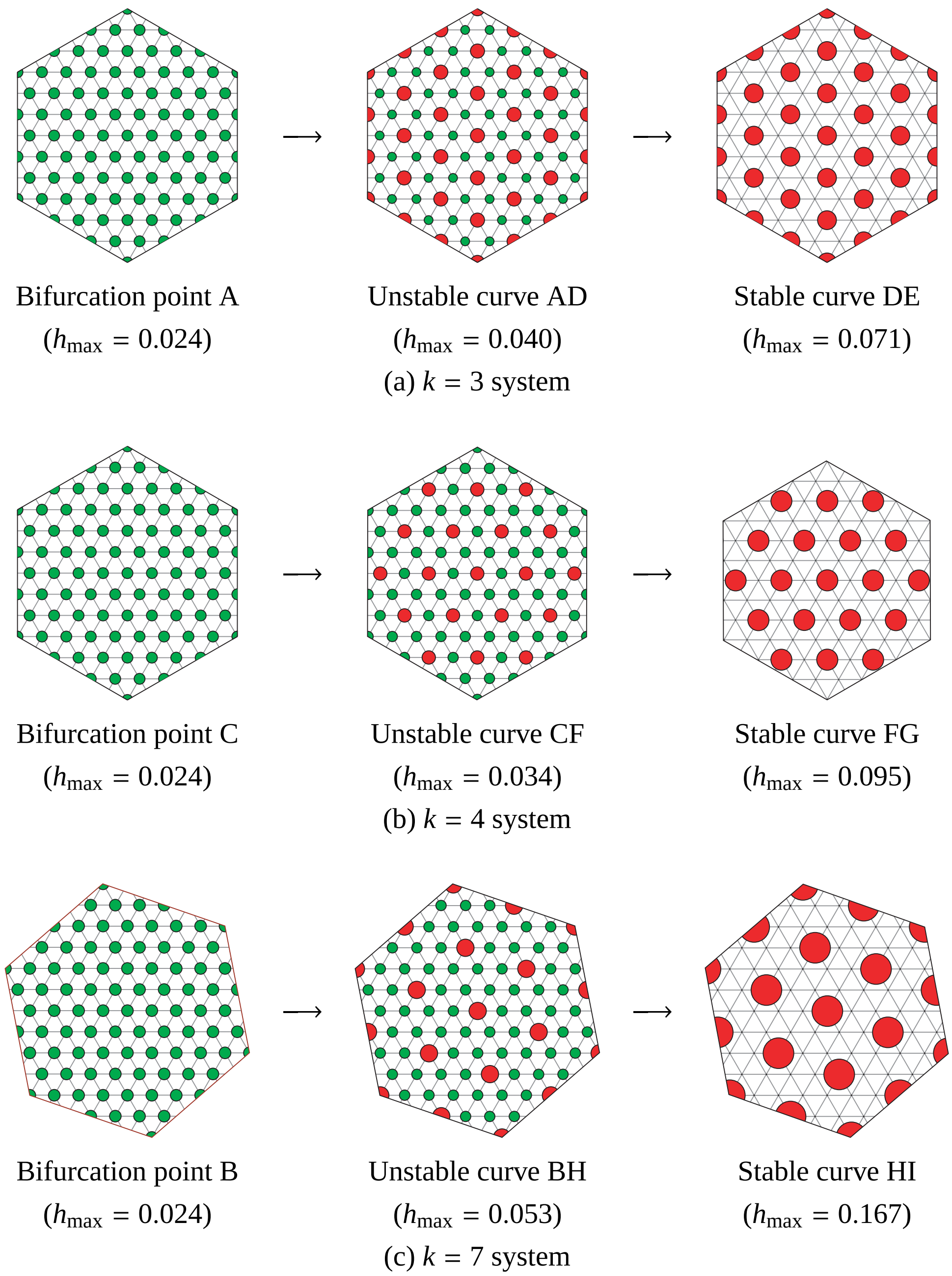

Figure 5: Change of population distributions observed along the bifurcated curves for $k = 3$, 4, and 7 systems for the FO model (the area of a circle represents the size of population of the associated place)

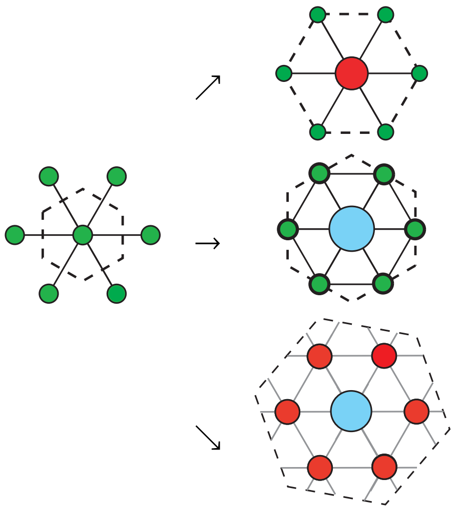

Figure 6: Enlargement of market areas for the first-level centers observed on the bifurcated curves associated with $k = 3, 4, 7$ systems (Hexagon drawn by the dashed lines denotes the market area)

The first-level centers, which are evenly scattered and are equidistant from each other with the distance $\sqrt{3}d$, form regular hexagons with the radius of $\sqrt{3}d$. This distribution, accordingly, is the $k = 3$ system with the (normalized) spatial period $T/d = \sqrt{3}$ in Fig. 3(b) ((25) in Proposition 3.1(iii)). The bifurcation at A is the spatial period $\sqrt{3}$-times bifurcation associated with

$$\begin{array}{cccc} T/d: & 1 & \to & \sqrt{3} \\ (\boldsymbol{t}_1, \boldsymbol{t}_2): & (\boldsymbol{\ell}_1, \boldsymbol{\ell}_2) & \to & (2\boldsymbol{\ell}_1 + \boldsymbol{\ell}_2, -\boldsymbol{\ell}_1 + \boldsymbol{\ell}_2) \\ \text{curve}: & \text{OO}' & \to & \text{ADE} \end{array}$$

Two neighboring first-level centers are connected by two kinked roads each of which passes a second-level center at the kink (Fig. 5(a)). Such formation of zigzag road between the two neighboring first-level centers is inferred in central place theory (Christaller, 1966, p.73, [9]).

The market area, in the sense of Remark 4.1 below, of a first-level center is the regular hexagon with the radius of d depicted at the upper right of Fig. 6 by the dashed lines. Each of the six second-level center is shared by three neighboring market areas; accordingly, $6/3 = 2$ second-level centers, in effect, belong to the market area. Hence the ratio of the number N_1 of the first-level centers to the number N_2 of the second-level centers is equal to $N_1 : N_2 = 1 : 2$ in agreement with the formula (18) for $k = 3$ of central place theory. Consequently, commonality exists between the computed population distribution for the core–periphery models and the prediction by central place theory, although they are based on different underpinnings.

Next, we shift eyes on the Pf model. Although the solution curves in Fig. 4(a) and (b) for the FO and Pf models showed differences in the shapes of the curves and locations of bifurcation points, the discussion above turned out to be applicable to the Pf model as well. In particular, the emergence of the $k = 3$ system is a general phenomenon that is independent of individual models. Such model independence is also demonstrated for $k = 4$ system in §4.2 and for $k = 7$ system in §4.3.

Remark 4.1. We consider a Voronoi decomposition (Okabe et al., 2000 [34]) of the two-dimensional domain for a system of first-level centers. Then the domain is decomposed into a set of identical hexagons. Each hexagon contains the first-level center at its center and six second-level centers surrounding the first-level center. Since the first-level center has the maximum market share to each of the second-level center, this hexagon can be regarded as the market area of the first-level center. It is to be noted, however, that for core–periphery models, the concept of market area is fictitious because the degrees of freedom are allocated only at the nodes of the hexagonal lattice. Yet, in this paper, this concept is used for convenience in the description of the progress of agglomeration. □

4.2 $k = 4$ system

For both models, bifurcated curves for $k = 4$ system branched at the triple bifurcation point C ($M = 3$) on the line OO′ for the uniform population (Fig. 4(a) and (b)). The bifurcated curve CFG of the FO model was unstable just after bifurcation (CF), and became stable during FG. The bifurcated curve CC′ of the Pf model was unstable throughout.

The progress of agglomeration observed on these bifurcated curves is shown in Fig. 5(b) for the FO model. (The Pf model displayed similar progress of agglomeration, but different stability.) Each first-level center is surrounded by six regular-hexagonal second-level centers. We can see straight lines of two kinds along the hexagonal grid. Some straight lines pass only second-level center. On each straight line passing first-level centers along the hexagonal grid, we can observe alternating of a first-level center and a second-level center, as is the case for the racetrack economy after the spatial period doubling bifurcation (Tabuchi and Thisse, 2011 [41], Akamatsu et al., 2009 [1], and Ikeda et al., 2010 [23]). Thus this agglomeration pattern can be touted as a two-dimensional counterpart of the spatial period doubling bifurcation in the racetrack economy.

The first level centers, which are evenly scattered and are equidistant from each other with the distance $\sqrt{4}d$, form regular hexagons with the radius of $\sqrt{4}d$. This distribution, accordingly, is the $k = 4$ system with the (normalized) spatial period $T/d = \sqrt{4}$ in Fig. 3(c) ((25) in Proposition 3.1(iii)). The bifurcation at C is the spatial period doubling bifurcation

$$\begin{array}{rccc} T/d: & 1 & \to & 2 \\ (\boldsymbol{t}_1, \boldsymbol{t}_2): & (\boldsymbol{\ell}_1, \boldsymbol{\ell}_2) & \to & (2\boldsymbol{\ell}_1, 2\boldsymbol{\ell}_2) \\ \text{curve}: & \text{OO}' & \to & \text{CFG or CC}' \end{array}$$

Although the bifurcated curves for the FO and Pf models have different stability, a bifurcated solution with the population distribution for the $k = 4$ system branched at the bifurcation point C in each model. The emergence of the $k = 4$ system, accordingly, is a general phenomenon that is independent of individual models.

Two neighboring first-level centers are connected by a straight road that passes a second-level center (Fig. 5(b)). This configuration agrees with Christaller's traffic principle for $k = 4$: "The traffic principle states that the distribution of central places is most favorable when as many important places as possible lie on one traffic route between two important towns, the route being as straightly and as cheaply as possible." (Christaller, 1966, p.74, [9]).

The market area, in the sense of Remark 4.1 above, of a first-level center is the regular hexagon depicted at the middle right of Fig. 6 by the dashed lines. Since each of the six second-level centers is shared by two neighboring market areas, $6/2 = 3$ second-level centers, in effect, exist in the market area. Hence the ratio of the number N_1 of the first-level centers to the number N_2 of the second-level centers is equal to $N_1 : N_2 = 1 : 3$ in agreement with the formula (18) for $k = 4$ of central place theory.

4.3 $k = 7$ system

For both models, a bifurcated curve BHI branched at the bifurcation point B of the multiplicity $M = 12$ on the line OO′ for the uniform population. The curve BHI lost stability at the onset of bifurcation, remained unstable during BH, regained stability at H, and remained stable during HI.

The progress of agglomeration observed on the bifurcated curve BHI is shown in Fig. 5(c) for the FO model. (The Pf model displayed similar progress of agglomeration.) Each first-level center is surrounded by six regular-hexagonal second-level centers. On each straight line along the hexagonal grid, we can observe repetitions of a first-level center and six second-level centers.

The first level centers, which are evenly scattered and are equidistant from each other with the distance $\sqrt{7}d$, form *tilted* regular hexagons with the radius of $\sqrt{7}d$. The emergence of such tilted hexagons is most phenomenal in the present study. This distribution, accordingly, is the $k = 7$ system with the (normalized) spatial period $T/d = \sqrt{7}$ in Fig. 3(d) ((25) in Proposition 3.1(iii)). The bifurcation at B is the spatial period $\sqrt{7}$-times bifurcation

$$\begin{array}{rccc} T/d: & 1 & \to & \sqrt{7} \\ (\boldsymbol{t}_1, \boldsymbol{t}_2): & (\boldsymbol{\ell}_1, \boldsymbol{\ell}_2) & \to & (3\boldsymbol{\ell}_1 - \boldsymbol{\ell}_2, -\boldsymbol{\ell}_1 + 2\boldsymbol{\ell}_2) \\ \text{curve}: & \text{OO}' & \to & \text{BHI} \end{array}$$

Although the solution curves in Fig. 4 for the FO and Pf models are apparently different, a bifurcated solution with the population distribution for the $k = 7$ system branched at the bifurcation point B in each model.

For the bifurcated curve BHI, the market area (Remark 4.1) of a first-level center is the regular hexagon depicted at the lower right of Fig. 6 by the dashed lines. Since the six second-level centers are entirely within the market area of the first-level center, the ratio of the number N_1 of the first-level centers to the number N_2 of the second-level centers is equal to $N_1 : N_2 = 1 : 6$. This agrees with Christaller's administrative principle for $k = 7$ system: "The ideal of such a spatial community has the nucleus as the capital (a central place of a higher rank), around it, a wreath of satellite places of lesser importance, and toward the edge of the region a thinning population density—and even uninhabited areas." (Christaller, 1966, p.77 [9]). It is restated, for short, by Dicken and Lloyd (1990, Chapter 1) [12] as "Lower-order centers are entirely within the hexagon of the higher-order center."

4.4 Dependence of stability of solutions on the transport cost

Up to now, we have investigated the emergence of Christaller's $k = 3, 4, 7$ systems. We now examine stable solutions, and investigate their dependence on the transport cost. As shown in Fig. 4, when the value of transport parameter τ is very large, the uniform population solution is the only stable solution and the solution curves for $k = 3, 4, 7$ systems are non-existent. When the transport parameter τ decreases, the uniform population solution becomes unstable at the bifurcation point A, and we can have the following rough observation for stable solutions of those systems:

- For the FO model, first the solutions for $k = 3$ system become stable at the point D, next those for $k = 7$ system become stable at the point H, and last those for $k = 4$ system become stable at the point F.
- For the Pf model, first the solutions for $k = 3$ system become stable at the point D, next those for $k = 7$ system become stable at the point H, and those for $k = 4$ system remain unstable throughout.

The solution curves for the $k = 3$ system, accordingly, are stable for larger τ values, but those for the $k = 7$ system are stable for smaller ones. The mechanism of such dependence of the stability on the transport cost might be explained from a standpoint of the tradeoff between transport costs and economies of scale:

- When the transport cost is high, the merit of the reduction of the transport cost becomes predominant in comparison with the merit of economies of scale. For this reason, the $k = 3$ system with a smaller market area is more efficient than the $k = 7$ system with a larger market area that demands more transport cost.
- When the transport cost is relatively small, the merit of economies of scale becomes predominant; accordingly, the $k = 7$ system with a larger market area is more efficient than the $k = 3$ system with a smaller market area.

Thus the dependence of the stability on the transport cost has economic necessity.

The curves for $k = 3$ and $k = 7$ systems are stable for wide range of the transport cost for both models. On the other hand, those for the $k = 4$ system are stable for relatively short range for the FO model, and unstable throughout for the Pf model. Such features are dependent on models, their parameter values, and the modeling of the transport cost in (8). It is a topic in future to untangle the economic mechanism of such stability by thorough studies of other important core–periphery models.

5 Conclusion

For a two-dimensional system modeled by core–periphery models of two kinds, self-organization of hexagonal population distributions for Christaller's three systems in central place theory is predicted by group-theoretic bifurcation theory, and their existence is verified and their stability is investigated by computational bifurcation analysis. It demonstrates inherent model-independent capability of the core–periphery models to express those systems provided with pertinent spatial platforms. Moreover, it confirms the prediction by Krugman (1996) [29] of the emergence of a system of hexagonal market areas in two dimensions, thereby paving the way for cross-fertilization between central place theory and new economic geography.

The agglomeration patterns for $k = 3$ system and $k = 7$ system are different from the pre-existing core–periphery patterns for the two-city model and racetrack economy. In contrast, the agglomeration pattern for $k = 4$ system can be touted as a two-dimensional counterpart of the spatial period doubling bifurcation in the racetrack economy. Such difference and similarity indicate the importance of the study of two-dimensional core–periphery patterns.

In central place theory, the three systems are explained based on market, traffic, and administrative principles. In contrast, the present analysis using the core–periphery models based on microeconomic underpinning engenders a hierarchy of different levels of centers without resort to these principles. The results obtained using central place theory must be reconsidered in light of economic geographical modeling to extend the horizon of core–periphery models.

Dependence of stability of solutions on the transport cost is investigated in view of economics of scales: When the transport cost is high, the $k = 3$ system with a smaller market area is more efficient than the $k = 7$ system. When it is small, the $k = 7$ system with a larger market area is more efficient. Thus the dependence of the stability on the transport cost has economic necessity.

Bifurcations are highlighted as a catalyst to break uniformity to engender the patterns. Group-theoretic bifurcation theory has displayed its usefulness to predict possible agglomeration patterns among a system of places in two dimensions, often associated with successive elongation of spatial periods. Information about symmetries of bifurcated solutions offered by this theory is important in choosing a bifurcation point that produces hexagonal distributions of interest.

Acknowledgment

Grant-in-Aid for Scientific Research (B) 19360227/21360194 is greatly acknowledged. This research is partially supported by the Aihara Project, the FIRST program from JSPS, initiated by CSTP.

A Group-theoretic bifurcation analysis on the $n \times n$ hexagonal lattice

In this Appendix, the mathematical aspects are given as an adaptation of Ikeda et al. (2011) [25]. Groups expressing the symmetry of the $n \times n$ hexagonal lattice are presented in §A.1. Group-theoretic bifurcation analysis for the core–periphery models is conducted in §A.2. Bifurcations that produce hexagonal distributions for Christaller's $k = 3$, 4, and 7 systems are studied in §A.3.

A.1 Groups expressing the symmetry

For the study of the agglomeration pattern of population distribution on the $n \times n$ hexagonal lattice, we use group-theoretic bifurcation theory: an established mathematical tool for investigating pattern formation. In this theory, the symmetries of possible bifurcated solutions are determined with resort to the group that labels the symmetry of the system. Hence the first step of the bifurcation analysis is to identify the underlying group.

A.1.1 Symmetry of the $n \times n$ hexagonal lattice

Symmetry of the $n \times n$ hexagonal lattice is characterized by invariance with respect to:

- r: counterclockwise rotation about the origin at an angle of $\pi/3$.
- s: reflection $y \mapsto -y$.
- p_1: periodic translation along the $\boldsymbol{\ell}_1$-axis (i.e., the x-axis).
- p_2: periodic translation along the $\boldsymbol{\ell}_2$-axis.

Consequently, the symmetry of the hexagonal lattice is described by the group

$$G = \langle r, s, p_1, p_2 \rangle, \tag{A.1}$$

where $\langle \cdots \rangle$ denotes a group generated by the elements therein, with the fundamental relations given by

$$\begin{aligned} r^6 &= s^2 = (rs)^2 = {p_1}^n = {p_2}^n = e, \\ rp_1 &= p_1 p_2 r, \quad rp_2 = p_1^{-1} r, \quad sp_1 = p_1 s, \quad sp_2 = p_1^{-1} p_2^{-1} s, \quad p_2 p_1 = p_1 p_2, \end{aligned}$$

where e is the identity element. Each element of G can be represented uniquely in the form of

$$s^l r^m {p_1}^i {p_2}^j, \quad i, j \in \{0, \ldots, n-1\};\ l \in \{0, 1\};\ m \in \{0, 1, \ldots, 5\}.$$

(For group theory, see Serre, 1977 [40].)

The group G contains the dihedral group $\langle r, s \rangle \simeq \mathrm{D}_6$ and cyclic groups $\langle p_1 \rangle \simeq \mathbb{Z}_n$ and $\langle p_2 \rangle \simeq \mathbb{Z}_n$ as its subgroups. Moreover, it has the structure of semidirect product of D_6 by $\mathbb{Z}_n \times \mathbb{Z}_n$, which is denoted as

$$G = \mathrm{D}_6 \dotplus (\mathbb{Z}_n \times \mathbb{Z}_n). \tag{A.2}$$

This means, in particular, that $\langle p_1, p_2 \rangle$ is a normal subgroup of G.

A.1.2 Subgroups

Among many subgroups of $G = \langle r, s, p_1, p_2\rangle = \mathrm{D}_6 \dotplus (\mathbb{Z}_n \times \mathbb{Z}_n)$, we are interested in those subgroups expressing the hexagons for Christaller's $k = 3$, 4, and 7 systems. Such subgroups G' are represented as the semidirect product of a subgroup G'_{local} of D_6 by a subgroup G'_{trans} of $\mathbb{Z}_n \times \mathbb{Z}_n$; i.e.,

$$G' = G'_{\mathrm{local}} \dotplus G'_{\mathrm{trans}}. \tag{A.3}$$

It should be clear that G'_{local} represents the local symmetry and G'_{trans} the translational symmetry. The local symmetry is given by

$$G'_{\mathrm{local}} = \begin{cases} \langle r, s\rangle & \text{for } k = 3, 4, \\ \langle r\rangle & \text{for } k = 7, \end{cases}$$

and the translational symmetry by

$$G'_{\mathrm{trans}} = \langle p_1^{\alpha} p_2^{\beta}, p_1^{-\beta} p_2^{\alpha-\beta}\rangle = \begin{cases} \langle p_1^2 p_2, p_1^{-1} p_2\rangle & \text{for } k = 3 \text{ system}, \\ \langle p_1^2, p_2^2\rangle & \text{for } k = 4 \text{ system}, \\ \langle p_1^3 p_2, p_1^{-1} p_2^2\rangle & \text{for } k = 7 \text{ system}. \end{cases}$$

See Table A.1. Accordingly, the subgroups for Christaller's $k = 3$, 4, 7 systems are

$$G' = G'_{\mathrm{local}} \dotplus G'_{\mathrm{trans}} = \begin{cases} \langle r, s\rangle \dotplus \langle p_1^2 p_2, p_1^{-1} p_2\rangle & \text{for } k = 3 \text{ system}, \\ \langle r, s\rangle \dotplus \langle p_1^2, p_2^2\rangle & \text{for } k = 4 \text{ system}, \\ \langle r\rangle \dotplus \langle p_1^3 p_2, p_1^{-1} p_2^2\rangle & \text{for } k = 7 \text{ system}. \end{cases} \tag{A.4}$$

From the translational symmetry we can derive a compatibility condition on the size n of the hexagonal lattice for a specified k value. For example,

- For $k = 3$ with $(\alpha, \beta) = (2, 1)$, we have $(p_1^2 p_2) \times (p_1^{-1} p_2)^{-1} = p_1^3$, which represents a translation in the direction of the $\boldsymbol{\ell}_1$-axis at the length of $3d$; accordingly, n must be a multiple of 3. The spatial period vectors are given by $(\boldsymbol{t}_1, \boldsymbol{t}_2) = (2\boldsymbol{\ell}_1 + \boldsymbol{\ell}_2, -\boldsymbol{\ell}_1 + \boldsymbol{\ell}_2)$. The spatial period elongates as $T/d = 1 \to \sqrt{3}\ (= \sqrt{k})$.

- For $k = 4$ with $(\alpha, \beta) = (2, 0)$, the symmetry of p_1^2 and p_2^2 implies that n is a multiple of 2. The spatial period vectors are given by $(\boldsymbol{t}_1, \boldsymbol{t}_2) = (2\boldsymbol{\ell}_1, 2\boldsymbol{\ell}_2)$. The spatial period elongates as $T/d = 1 \to \sqrt{4}\ (= \sqrt{k})$.

- For $k = 7$ with $(\alpha, \beta) = (3, 1)$, we have $(p_1^3 p_2)^2 \times (p_1^{-1} p_2^2)^{-1} = p_1^7$, from which follows that n is a multiple of 7. The spatial period vectors are given by $(\boldsymbol{t}_1, \boldsymbol{t}_2) = (3\boldsymbol{\ell}_1 + \boldsymbol{\ell}_2, -\boldsymbol{\ell}_1 + 2\boldsymbol{\ell}_2)$. The spatial period elongates as $T/d = 1 \to \sqrt{7}\ (= \sqrt{k})$.

A.2 Exploiting symmetry of core–periphery models by group-theoretic bifurcation theory

For investigation of the patterns of the bifurcated solutions, it is crucial to formulate the symmetry that is inherent in the governing equation in (16):

$$\boldsymbol{F}(\boldsymbol{h}, \tau) = H\boldsymbol{P}(\boldsymbol{h}) - \boldsymbol{h} = \boldsymbol{0}. \tag{A.5}$$

Table A.1: The values of (α,β), tilted angle φ, local and translational symmetries, and compatible n for Christaller's $k = 3$, 4, and 7 systems

k	(α,β)	Tilted angle φ	Local symmetry G'_{local}	Translational symmetry G'_{trans}	Lattice size n $(m = 1, 2, \ldots)$
3	$(2,1)$	$\pi/6$	$\langle r, s\rangle$	$\langle p_1^2 p_2, p_1^{-1} p_2\rangle$	$3m$
4	$(2,0)$	0	$\langle r, s\rangle$	$\langle p_1^2, p_2^2\rangle$	$2m$
7	$(3,1)$	0.106π	$\langle r\rangle$	$\langle p_1^3 p_2, p_1^{-1} p_2^2\rangle$	$7m$

In group-theoretic bifurcation theory, the symmetry of the equation for the system of $n \times n$ places on the hexagonal lattice is described as

$$T(g)\boldsymbol{F}(\boldsymbol{h},\tau) = \boldsymbol{F}(T(g)\boldsymbol{h},\tau), \quad g \in G, \tag{A.6}$$

in terms of an orthogonal matrix representation T of group $G = \langle r, s, p_1, p_2\rangle$ in (A.1) on the K-dimensional space $\mathbb{R}^K$. The condition (or property) (A.6) is called the equivariance of $\boldsymbol{F}(\boldsymbol{h},\tau)$ to G. The most important consequence of the equivariance (A.6) is that the symmetries of the whole set of possible bifurcated solutions can be obtained and classified.

In our study of a system of $n \times n$ places in the hexagonal lattice, each element g of G acts as a permutation of place numbers $(1,\ldots,K)$ for $K = n^2$ and hence each $T(g)$ is a permutation matrix. Then we can show the equivariance (A.6) to $G = \langle r, s, p_1, p_2\rangle$ of the core–periphery models as below.
Proof. By expressing the action of $g \in G$ as $g: i \mapsto i^*$ for place numbers i and i^*, we have $v_i(T(g)\boldsymbol{h},\tau) = v_{i^*}(\boldsymbol{h},\tau)$ and $P_i(T(g)\boldsymbol{h},\tau) = P_{i^*}(\boldsymbol{h},\tau)$ by (15) for any $g \in G$. Therefore, we have

$$\begin{aligned} F_i(T(g)\boldsymbol{h},\tau) &= HP_i(T(g)\boldsymbol{h},\tau) - h_{i^*} \\ &= HP_{i^*}(\boldsymbol{h},\tau) - h_{i^*} \\ &= F_{i^*}(\boldsymbol{h},\tau). \end{aligned}$$

This proves the equivariance (A.6). □

According to group-theoretic bifurcation theory the (bifurcation) analysis proceeds as follows. Consider, to be specific, a critical point $(\boldsymbol{h}_{\rm c},\tau_{\rm c})$ of multiplicity $M\,(\geq 1)$, at which the Jacobian matrix of $\boldsymbol{F}$ has M zero eigenvalues.

With the use of a standard procedure called the *Liapunov–Schmidt reduction with symmetry* (Sattinger, 1979 [39]; Golubitsky et al., 1988 [21]), the full system of equations (A.5) is reduced, in a neighborhood of $(\boldsymbol{h}_{\rm c},\tau_{\rm c})$, to a system of M equations (called bifurcation equations)

$$\widetilde{\boldsymbol{F}}(\boldsymbol{w},\widetilde{\tau}) = \boldsymbol{0} \tag{A.7}$$

in $\boldsymbol{w} \in \mathbb{R}^M$, where $\widetilde{\boldsymbol{F}}: \mathbb{R}^M \times \mathbb{R} \to \mathbb{R}^M$ is a function and $\widetilde{\tau} = \tau - \tau_{\rm c}$ denotes the increment of τ. In this reduction process the equivariance of the full system, which is formulated in (A.6), is inherited by the reduced system (A.7) in the following form:

$$\widetilde{T}(g)\widetilde{\boldsymbol{F}}(\boldsymbol{w},\widetilde{\tau}) = \widetilde{\boldsymbol{F}}(\widetilde{T}(g)\boldsymbol{w},\widetilde{\tau}), \qquad g \in G, \tag{A.8}$$

Table A.2: Number N_d of d-dimensional irreducible representations of $\mathrm{D}_6 \dot{+} (\mathbb{Z}_n \times \mathbb{Z}_n)$

$n \setminus d$	1	2	3	4	6	12
	N_1	N_2	N_3	N_4	N_6	N_{12}
$6m$	4	4	4	1	$2n-6$	$(n^2-6n+12)/12$
$6m \pm 1$	4	2	0	0	$2n-2$	$(n^2-6n+5)/12$
$6m \pm 2$	4	2	4	0	$2n-4$	$(n^2-6n+8)/12$
$6m \pm 3$	4	4	0	1	$2n-4$	$(n^2-6n+9)/12$

where $\widetilde{T}$ is the subrepresentation of T on the M-dimensional kernel space of the Jacobian matrix. It is this inheritance of symmetry that plays a key role in determining the symmetry of bifurcating solutions.

The reduced equation (A.7) is to be solved for $\boldsymbol{w}$ as $\boldsymbol{w} = \boldsymbol{w}(\widetilde{\tau})$, which is often possible by virtue of the symmetry of $\widetilde{\boldsymbol{F}}$ described in (A.8). Since $(\boldsymbol{w}, \widetilde{\tau}) = (\boldsymbol{0}, 0)$ is a singular point of (A.7), there can be many solutions $\boldsymbol{w} = \boldsymbol{w}(\widetilde{\tau})$ with $\boldsymbol{w}(0) = \boldsymbol{0}$, which gives rise to bifurcation. Each $\boldsymbol{w}$ uniquely determines a solution $\boldsymbol{h}$ of the full system (A.5).

The symmetry of $\boldsymbol{h}$ is represented by a subgroup of G defined by

$$\Sigma(\boldsymbol{h}; G, T) = \{g \in G \mid T(g)\boldsymbol{h} = \boldsymbol{h}\}, \tag{A.9}$$

called the isotropy subgroup of $\boldsymbol{h}$. The isotropy subgroup $\Sigma(\boldsymbol{h})$ can be computed in terms of the symmetry of the corresponding $\boldsymbol{w}$ as

$$\Sigma(\boldsymbol{h}; G, T) = \Sigma(\boldsymbol{w}; G, \widetilde{T}), \tag{A.10}$$

where

$$\Sigma(\boldsymbol{w}; G, \widetilde{T}) = \{g \in G \mid \widetilde{T}(g)\boldsymbol{w} = \boldsymbol{w}\}. \tag{A.11}$$

The relation (A.10) enables us to determine the symmetry of bifurcated solutions $\boldsymbol{h}$ through the analysis of bifurcation equations in $\boldsymbol{w}$.

A.3 Theoretically predicted hexagonal distributions

Possible bifurcated solutions of the governing equation (A.5) for uniformly distributed population solution representing hexagonal distributions are predicted by group-theoretic bifurcation theory.

The multiplicity M of critical points (i.e., the dimension of the kernel space of the Jacobian matrix of $\boldsymbol{F}$ in (A.5) at bifurcation points) is generically either 1, 2, 3, 4, 6, or 12, which is a natural consequence of the group-theoretic fact that the dimension d of an irreducible representation of the group G is either $d = 1, 2, 3, 4, 6$, or 12. The numbers N_d of the d-dimensional irreducible representations are listed in Table A.2.

We present a possible bifurcation mechanism that can produce hexagonal distributions of population of skilled workers associated with Christaller's $k = 3, 4$, and 7 systems expressed by the subgroups in (A.4). The main message is that such bifurcated solutions do exist, and therefore these systems can be understood within the framework of group-theoretic bifurcation theory. The hexagonal distributions for Christaller's $k = 3$, 4, and 7 systems emerge from bifurcation points of multiplicity $M = 2$, 3, 12, respectively, but not of $M = 1$, 4, 6. It is mentioned in particular that the distributions for Christaller's $k = 7$ system are associated with "simple hexagons" in Dionne, Silber, and Skeldon (1997) [13].

A.3.1 Analysis by equivariant branching lemma

The emergence of Christaller's hexagons is proved by applying the equivariant branching lemma to the bifurcation equation $\widetilde{\boldsymbol{F}}(\boldsymbol{w}, \widetilde{\tau})$ in (A.7); see, e.g., Golubitsky, Stewart, and Schaeffer (1988) [21] for this lemma. Recall that bifurcation equation is associated with an irreducible representation of G and that the isotropy subgroup $\Sigma(\boldsymbol{h})$ in (A.9) expressing the symmetry of a bifurcated solution $\boldsymbol{h}$ is identical with the isotropy subgroup $\Sigma(\boldsymbol{w})$ in (A.11) of the corresponding solution $\boldsymbol{w}$ for the bifurcation equation, i.e., $\Sigma(\boldsymbol{h}) = \Sigma(\boldsymbol{w})$ as shown in (A.10). A subgroup Σ is said to be an isotropy subgroup if $\Sigma = \Sigma(\boldsymbol{h})$ for some $\boldsymbol{h}$.

The analysis based on the equivariant branching lemma proceeds as follows:

- Specify an isotropy subgroup Σ of G for the symmetry of a possible bifurcated solution as well as an irreducible representation $\widetilde{T}$ of G that can possibly be associated with the bifurcation point.
- Obtain the fixed-point subspace $\mathrm{Fix}(\Sigma)$ for the isotropy subgroup Σ with respect to the irreducible representation $\widetilde{T}$, where

$$\mathrm{Fix}(\Sigma) = \{\boldsymbol{w} \in \mathbb{R}^M \mid \widetilde{T}(g)\boldsymbol{w} = \boldsymbol{w} \text{ for all } g \in \Sigma\}. \tag{A.12}$$

- Calculate the dimension $\dim \mathrm{Fix}(\Sigma)$ of this subspace.
- If $\dim \mathrm{Fix}(\Sigma) = 1$, a bifurcated solution with symmetry Σ is guaranteed to exist generically by the equivariant branching lemma. If $\dim \mathrm{Fix}(\Sigma) = 0$, a bifurcated solution with symmetry Σ is non-existent. If $\dim \mathrm{Fix}(\Sigma) \geq 2$, no definite conclusion can be reached by the equivariant branching lemma.

Isotropy subgroups with $\dim \mathrm{Fix}(\Sigma) = 1$ are called *axial subgroups* and the associated spatially doubly periodic solutions are called *axial planforms* (Golubitsky, Dionne, and Stewart, 1994 [19]).

In our present analysis, we employ the above procedure with $\Sigma = G'$ for each G' in (A.4) and for each irreducible representation $\widetilde{T}$ of G; note that each G', representing the symmetry of a Christaller's hexagon, is an isotropy subgroup. Since the dimension of $\widetilde{T}$ is either $d = 1$, 2, 3, 4, 6, or 12, the multiplicity M of the critical point is generically either 1, 2, 3, 4, 6, or 12. The equivalent branching lemma applies only if $\dim \mathrm{Fix}(\Sigma) = 1$. Fortunately, it will turn out (see §A.3.2 to §A.3.4) that, in all cases of our interest in (A.4), we have $\dim \mathrm{Fix}(\Sigma) \leq 1$ and therefore we can always rely on the equivalent branching lemma to determine the existence or nonexistence of bifurcated solutions for Christaller's hexagons.

A.3.2 $k = 3$ system

When n is a multiple of 3, hexagons for Christaller's $k = 3$ system appear generically as a branch from a bifurcation point that is associated with the irreducible representation given by

$$T(r) = \begin{bmatrix} 1 & 0 \\ 0 & -1 \end{bmatrix},\ T(s) = \begin{bmatrix} 1 & 0 \\ 0 & 1 \end{bmatrix},\ T(p_1) = T(p_2) = \begin{bmatrix} \cos 2\pi/3 & -\sin 2\pi/3 \\ \sin 2\pi/3 & \cos 2\pi/3 \end{bmatrix}. \tag{A.13}$$

This is one of the four two-dimensional irreducible representations of $D_6 \dotplus (\mathbb{Z}_n \times \mathbb{Z}_n) = \langle r, s, p_1, p_2 \rangle$ (Table A.2). Since this is two-dimensional, the multiplicity of the bifurcation point is $M = 2$.

The general procedure in Section A.3.1 is applied to

$$\Sigma = \langle r, s, p_1^2 p_2, p_1^{-1} p_2 \rangle = \langle r, s \rangle \dotplus \langle p_1^2 p_2, p_1^{-1} p_2 \rangle, \tag{A.14}$$

which describes the symmetry of the hexagon for Christaller's $k = 3$ system in Fig. 3(b). The fixed-point subspace Fix(Σ) with respect to $\widetilde{T} = T$ in (A.13) is a one-dimensional subspace of $\mathbb{R}^2$ spanned by $(1, 0)^\top$. Then, by the equivariant branching lemma, there exists a bifurcated path with the symmetry of (A.14).

This is a hexagonal distribution with the spatial period vectors

$$(\boldsymbol{t}_1, \boldsymbol{t}_2) = (2\boldsymbol{\ell}_1 + \boldsymbol{\ell}_2, -\boldsymbol{\ell}_1 + \boldsymbol{\ell}_2),$$

which corresponds to $(\alpha, \beta) = (2, 1)$ in (21). The symmetries $p_1^2 p_2$ and $p_1^{-1} p_2$ are apparent from this expression. The spatial period elongates as $T/d = 1 \to \sqrt{3}$, in agreement with central place theory ((17) for $k = 3$).

A.3.3 $k = 4$ system

When n is a multiple of 2, hexagonal patterns for the $k = 4$ system are predicted using group-theoretic bifurcation analysis to branch from a bifurcation point that is associated with the irreducible representation of G given as

$$T(r) = \begin{bmatrix} 0 & 1 & 0 \\ 0 & 0 & 1 \\ 1 & 0 & 0 \end{bmatrix}, \quad T(s) = \begin{bmatrix} 1 & 0 & 0 \\ 0 & 0 & 1 \\ 0 & 1 & 0 \end{bmatrix}; \tag{A.15}$$

$$T(p_1) = \begin{bmatrix} 1 & 0 & 0 \\ 0 & -1 & 0 \\ 0 & 0 & -1 \end{bmatrix}, \quad T(p_2) = \begin{bmatrix} -1 & 0 & 0 \\ 0 & 1 & 0 \\ 0 & 0 & -1 \end{bmatrix}. \tag{A.16}$$

This corresponds to one of the four three-dimensional irreducible representations of $D_6 \dotplus (\mathbb{Z}_n \times \mathbb{Z}_n) = \langle r, s, p_1, p_2 \rangle$ (Table A.2). Since this is three-dimensional, the multiplicity of the bifurcation point is $M = 3$.

The general procedure in Section A.3.1 is applied to

$$\Sigma = \langle r, s, p_1^2, p_2^2 \rangle = \langle r, s \rangle \dotplus \langle p_1^2, p_2^2 \rangle \simeq D_6 \dotplus (\mathbb{Z}_{n/2} \times \mathbb{Z}_{n/2}), \tag{A.17}$$

which expresses the symmetry of the hexagon for Christaller's $k = 4$ system in Fig. 3(c). The fixed-point subspace Fix(Σ) with respect to $\widetilde{T} = T$ in (A.15) and (A.16) is a one-dimensional subspace of $\mathbb{R}^3$ spanned by $(1, 1, 1)^\top$. Then, by the equivariant branching lemma, there exists a bifurcated path with the symmetry of (A.17).

This is a hexagonal distribution with the spatial period vectors

$$(\boldsymbol{t}_1, \boldsymbol{t}_2) = (2\boldsymbol{\ell}_1, 2\boldsymbol{\ell}_2),$$

which corresponds to $(\alpha, \beta) = (2, 0)$ in (21). The symmetries p_1^2 and p_2^2 are apparent from this expression. The spatial period elongates as $T/d = 1 \to \sqrt{4}$, in agreement with central place theory ((17) for $k = 4$).

A.3.4 $k = 7$ system

When n is a multiple of 7, hexagonal patterns for $k = 7$ system are predicted to branch by group-theoretic bifurcation analysis for the group $\mathrm{D}_6 \dot{+} (\mathbb{Z}_n \times \mathbb{Z}_n)$ at a bifurcation point associated with a 12-dimensional irreducible representation. Since this is 12-dimensional, the multiplicity of the bifurcation point is $M = 12$. There is a bifurcated solution with the symmetry (Ikeda et al., 2011 [25])

$$\langle r, p_1^3 p_2, p_1^{-1} p_2^2 \rangle = \langle r \rangle \dot{+} \langle p_1^3 p_2, p_1^{-1} p_2^2 \rangle = \langle r \rangle \dot{+} \langle p_1^3 p_2, p_1^7 \rangle \simeq \mathrm{C}_6 \dot{+} (\mathbb{Z}_n \times \mathbb{Z}_{n/7}). \quad \text{(A.18)}$$

By (A.4), this solution is associated with the tilted hexagon for $k = 7$ system in Fig. 3(d). The emergence of this solution is also demonstrated in the computational bifurcation analysis for $n = 42$ in §4.3.

This is a hexagonal distribution with the spatial period vectors

$$(\boldsymbol{t}_1, \boldsymbol{t}_2) = (3\boldsymbol{\ell}_1 + \boldsymbol{\ell}_2, -\boldsymbol{\ell}_1 + 2\boldsymbol{\ell}_2),$$

which corresponds to $(\alpha, \beta) = (3, 1)$ in (21). The symmetries $p_1^3 p_2$ and $p_1^{-1} p_2^2$ are apparent from this expression. The spatial period elongates as $T/d = 1 \to \sqrt{7}$, in agreement with central place theory ((17) for $k = 7$).

References

[1] T. Akamatsu, Y. Takayama, K. Ikeda, Spatial discounting, Fourier, and racetrack economy: A recipe for the analysis of spatial agglomeration models, Preprint: *MPRA Paper* 21738, University Library of Munich, Germany, 2009.

[2] S. P. Anderson, A. de Palma, J. F. Thisse, *Discrete Choice Theory of Product Differentiation*, MIT Press, 1992.

[3] R. Baldwin, R. Forslid, P. Martin, G. Ottaviano, F. Robert-Nicoud, *Economic Geography and Public Policy*, Princeton University Press, 2003.

[4] K. S. O. Beavon, *Central Place Theory: A Reinterpretation*, Longman, 1977.

[5] K. Behrens, J.-F. Thisse, Regional economics: A new economic geography perspective. *Regional Science and Urban Economics* 37(4) (2007) 457–465.

[6] M. Bosker, S. Brakman, H. Garretsen, M. Schramm, Adding geography to the new economic geography: bridging the gap between theory and empirics. *Journal of Economic Geography* 10 (2010) 793–823; doi: 10.1093/jeg/lbq003.

[7] S. Brakman, H. Garretsen, C. van Marrewijk, *The New Introduction to Geographical Economics*, Cambridge University Press; 2nd ed., 2009.

[8] E. Buzano, M. Golubitsky, Bifurcation on the hexagonal lattice and the planar Bénard problem. *Philosophical Transactions of the Royal Society of London* A 308 (1983) 617–667.

[9] W. Christaller, *Central Places in Southern Germany*, Prentice Hall, 1966.

[10] M. Clarke, A. G. Wilson, The dynamics of urban spatial structure: The progress of a research programme, *Transactions of the Institute of British Geographers, New Series* 10(4) (1985) 427–451.

[11] P. P. Combes, T. Mayer, J. F. Thisse, *Economic Geography: The Integration of Regions and Nations*, Princeton University Press, 2008.

[12] P. Dicken, P. E. Lloyd, *Location in Space: Theoretical Perspectives in Economic Geography*, 3rd ed., Harper Collins, 1990.

[13] B. Dionne, M. Silber, A. C. Skeldon, Stability results for steady, spatially, periodic planforms, *Nonlinearity* 10 (1997) 321–353.

[14] A. Dixit, J. Stiglitz, Monopolistic competition and optimum product diversity, *American Economic Review* 67 (1977) 297–308.

[15] H. Flam, E. Helpman, Industrial policy under monopolistic competition, *Journal of International Economics* 22 (1987) 79-102.

[16] R. Forslid, G. I. P. Ottaviano, An analytically solvable core-periphery model, *Journal of Economic Geography* 3 (2003) 229–340.

[17] D. Fudenberg, D. K. Levine, *The Theory of Learning in Games*, MIT Press, 1998.

[18] M. Fujita, P. Krugman, A. J. Venables, *The Spatial Economy: Cities, Regions, and International Trade*, MIT Press, 1999.

[19] M. Golubitsky, B. Dionne, I. Stewart, Coupled-cells, wreath products and direct products, in: *Dynamics, Bifurcations, Symmetry*, ed. P. Chossat (Kluwer, Dordrecht) 127–138, 1994.

[20] M. Golubitsky, I. Stewart, *The Symmetry Perspective*, Birkhäuser Verlag, 2002.

[21] M. Golubitsky, I. Stewart, D. G. Schaeffer, *Singularities and Groups in Bifurcation Theory*, Vol. 2, Springer-Verlag, 1988.

[22] J. Hofbauer, W. H. Sandholm, Evolution in games with randomly disturbed payoffs, *Journal of Economic Theory* 132 (2007) 47–69.

[23] K. Ikeda, T. Akamatsu, T. Kono, Spatial period-doubling agglomeration of a core–periphery model with a system of cities, Preprint: *MPRA Paper* 25636, University Library of Munich, Germany, 2010.

[24] K. Ikeda, K. Murota, *Imperfect Bifurcation in Stuctures and Materials*, 2nd ed., Springer-Verlag, 2010.

[25] K. Ikeda, K. Murota, T. Akamatsu, Self-organization of Lösch's hexagons in economic agglomeration for core–periphery models, *Technical Report: METR*, Dept. Math. Informatics, Univ. Tokyo 2011–15, 2011: To appear in *International Journal of Bifurcation and Chaos*.

[26] W. Isard, *Introduction to Regional Science*, Prentice-Hall, 1975.

[27] P. Krugman, Increasing returns and economic geography, *Journal of Political Economy* 99 (1991) 483–499.

[28] P. Krugman, On the number and location of cities, *European Economic Review* 37 (1993) 293–298.

[29] P. Krugman, *The Self-Organizing Economy*, Blackwell, 1996.

[30] A. Lösch, *The Economics of Location*, Yale University Press, 1954.

[31] P. J. Martin, C. A. Rogers, Trade Effects of Regional Aid, in Baldwin, R., Haaparanta, P. and Kiander, J. (eds.), *Expanding Membership of the European Union*, Cambridge University Press, 166–188, 1995.

[32] D. McFadden, Conditional Logit Analysis of Qualitative Choice Behavior, in Zarembka, P. (ed.), *Frontiers in Econometrics*, Academic Press, 105–142, 1974.

[33] M. Munz and W. Weidlich, Settlement formation, Part II: Numerical simulation, *The Annals of Regional Science* 24 (1990) 177–196.

[34] A. Okabe, B. Boots, K. Sugihara, S. N. Chiu, *Spatial Tessellations: Concepts and Applications of Voronoi Diagrams*, 2nd ed., Wiley, 2000.

[35] M. Pflüger, A simple, analytically solvable, chamberlinian agglomeration model, *Regional Science and Urban Economics* 34 (2004) 565–573.

[36] P. M. Picard, T. Tabuchi, Self-organized agglomerations and transport costs, *Economic Theory* 42 (2010) 565–589.

[37] W. H. Sandholm, *Population Games and Evolutionary Dynamics*, MIT Press, 2010.

[38] D. H. Sattinger, Group representation theory, bifurcation theory and pattern formation, *J. Funct. Anal.* 28 (1978) 58–101.

[39] D. H. Sattinger, *Group Theoretic Methods in Bifurcation Theory*, Springer-Verlag, 1979.

[40] J.-P. Serre, *Linear Representations of Finite Groups*, Springer-Verlag, 1977.

[41] T. Tabuchi, J. F. Thisse, A new economic geography model of central places. *Journal of Urban Economics* 69 (2011) 240–252.